Ground Reaction Forces Generated by Runners—Harmonic Analyses and Modelling

Marek Pańtak [ID]

Faculty of Civil Engineering, Division of Bridge, Metal and Timber Structures, Cracow University of Technology, 31-155 Kraków, Poland; marek.pantak@pk.edu.pl; Tel.: +48-12-628-29-13

check for updates

Featured Application: The presented topic is applicable during the dynamic analysis of pedestrian-carrying structures exposed to the dynamic action of runners. The presented information enables the prediction of the dynamic response of the structure and verification of the serviceability limit state of vibration in terms of the comfort of use of the structure.

Abstract: Building structures carrying pedestrian traffic, e.g., footbridges, long-span floors and long cantilevered platforms projecting outwards from the walls (long balconies), can be susceptible to the dynamic influence of its users. One type of dynamic action that can occur on these structures is the dynamic action of people running. The main aim of this paper is to present the results of the harmonic analyses and mathematical models of two types of ground reaction forces (*GRFs*) generated by people applying different running techniques, i.e., forefoot- and heel-strike (rearfoot) running technique. The analyses of the *GRFs* were performed on the basis of the results of laboratory tests of running people and concern the vertical component of the ground reaction forces (*VGRFs*) generated by runners. The harmonic analyses were performed using Fourier transform. The results of the study show the main features and differences between forces generated by forefoot- and heel-strike runners. Data obtained for various running styles allowed the development of a load model proposal for the *VGRFs* generated by heel-strike runners. The results of the *VGRF* parameterization and the proposed new *VGRF* model allow the *VGRFs* generated by forefoot and heel-strike runners to be accurately estimated in the case of normal running pace (recreational running). The application of the presented results allows improvements to the accuracy of determining the dynamic response of structures induced by runners.

Keywords: footbridge vibration; vibration serviceability; running; ground reaction forces; forefoot-strike; heel-strike; rearfoot-strike

---

1. Introduction

The specificity of designing building structures requires verification of the serviceability limit states, including vibration caused by foot traffic. In order to verify the requirements of vibration serviceability limit states, appropriate design scenarios should be selected depending on the types of foot traffic that can occur on the structure during its service life. The type of foot traffic strongly depends on the main aim of the foot traffic and location of the structure. In buildings and city areas where the probability of people hurrying or exercising is high, the structures can be exposed to the action of people running. Examples of these structures are footbridges located within recreational areas (city parks, walking boulevards, etc.) or located in the vicinity of public transport stops or public transport hubs. Runners can induce excessive vibration of these structures, which can significantly disturb the comfort of its use. Excessive vibration of footbridges can also be induced by runners during sporting events (half marathons, marathons, running trainings, etc.). Cases of excessive vibration of

footbridges induced by running people have been reported in [1–8]. In the case of steel footbridges, one running person can induce high amplitude vibration acceleration reaching 2.0–3.0 m/s^2 or more [3]. At the design stage of these structures, dynamic loads generated by people running should be taken into account where relevant.

Ground reaction forces generated during running depends on the running technique, which manifests itself in different foot-ground contact patterns (foot-strike patterns). Detailed analysis of the run allows the identification of three types of foot contact with the ground: heel-strike pattern (also known as a rearfoot-strike pattern), in which the heel contacts with the ground first; midfoot-strike pattern, in which the heel and the forefoot (the ball of the foot) make contact with the ground simultaneously; and forefoot-strike pattern in which the forefoot contacts the ground first (the heel does not touch the ground). Different types of foot-strike patterns produce a different time course of the ground reaction force (*GRF*). In Figure 1, the time courses of the vertical component of normalised ground reaction forces ($F_{VGRF} = VGRF/G$, where: G—weight of running person) for different foot-striking patterns are presented.
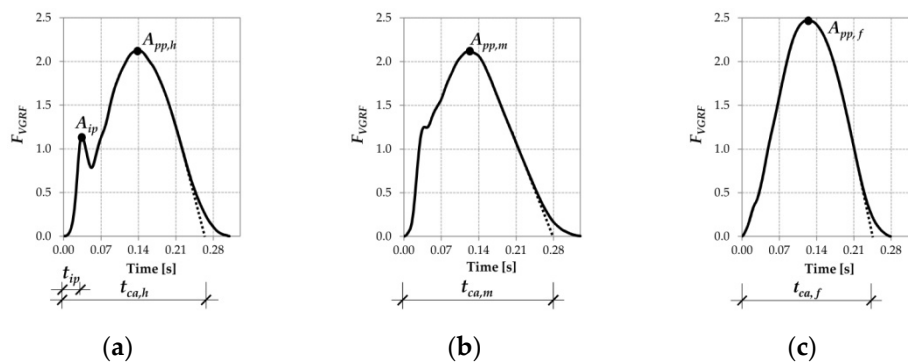

(a) (b) (c)

Figure 1. Examples of time courses of normalised ground reaction forces F_{VGRF} for different foot-strike patterns for running frequency $f_r = 2.80$ Hz: (**a**) heel-strike pattern, (**b**) midfoot-strike pattern, (**c**) forefoot-strike pattern (based on the author's research results).

The *VGRF* generated by a heel-strike runner is characterised by two peaks: an impact peak (A_{ip}) and a propulsive peak (A_{pp}). During forefoot-strike running, only propulsive peak A_{pp} occurs in the course of the *VGRF*. Midfoot-strike running is an intermediate case in which only a small impact peak may occur in the course of the *VGRF*. The most important differences between the course of the *VGRFs* for different foot-strike patterns concern the value of amplitudes of propulsive peak and the value of contact time (see Sections 3 and 4 for details).

There are several proposals for mathematical models of the *VGRF* generated by a running person in the literature [8–14]. All of these models allow the *VGRF* generated to be determined during the forefoot-strike running technique, i.e., the *VGRF* not containing the impact peak A_{ip}. In [9–12] the Fourier series was used to describe the *VGRF* time course. It is worth noting that parameters of the Fourier series presented in [9–11] enable correct estimation of the *VGRF* for an ordinary running activity with step frequency $f_r = 2.0$–4.0 Hz, while the application of the Fourier coefficients proposed in [12] leads to an overestimation of the *VGRF* amplitude (detailed analyses of this topic are presented in [15]). In addition, models presented in [9–12] recommend the use of 3 or 4 harmonics to determine the *VGRF* curve. For frequency of running $f_r = 2.80$ Hz (the typical pace of running), the frequency range corresponding to 4 harmonics is 2.8–11.0 Hz. These proposals can be considered correct for modelling the *VGRF* generated during forefoot running for the needs of dynamic analysis performed in civil engineering tasks. To determine the *VGRF* generated by heel-strike runners, consideration of approximately 10–15 harmonics is required [16,17]. For a frequency of running of $f_r = 2.80$ Hz the frequency range corresponding to 15 harmonics is 2.8–45.0 Hz (see Section 4 for details).

Another type of the *VGRF* model, called the half-sine model, has been proposed in [7,13]. The half-sine model allows determination of the *VGRF* generated during the forefoot-strike running technique. It should be also mentioned that the half-sine model is very sensitive to the value of contact time of the foot with the ground t_c. The amplitude of the *VGRF* in the half-sine model is inversely proportional to t_c. The assumption of the underestimated t_c, e.g., $t_c = 0.5\ T_r$ recommended in [7] for ordinary running activity (where: T_r—running period, $T_r = 1/f_r$), results in a large overestimation of the *VGRF* amplitude [1,15] (see Section 4 for details).

The load model proposed in [14] is another example of a model of the *VGRF* generated by a runner, enabling determination of the *VGRF* in the form of a half-sine curve. The model allows the reliable value of the dynamic response of the structure subjected to the dynamic action of running people to be estimated, but it cannot be directly compared with the measured *VGRFs*. The model is characterized by a constant amplitude of 1250 N, as well as the duration of the foot contact time with the ground being significantly shorter than contact time values measured during running tests. The model proposed in [14] describes the force which generates an impulse causing a dynamic response of the structure comparable to the response induced by real *VGRFs*, but the parameters of the modelled *VGRFs* are not directly comparable to the parameters of the measured *VGRFs*.

A different methodology for the *VGRF* modelling, presented in [18], uses the sum of the Gaussian functions to reconstruct the *VGRF* time course. The proposed procedure does not distinguish between running techniques but can easily be adapted to model different running styles. The correct selection of the number and parameters of the Gaussian functions enables determination of the template curve of the *VGRF* separately for forefoot-strike and heel-strike running.

Another method of the *VGRF* modelling has been presented in [19,20]. In the model, the runner's body was divided into two masses: m_1—the mass of the lower limb which contacts with the ground during running ($m_1 = 0.08\ G$, where: G—total body mass of the runner)—and m_2—the mass of the rest of the runner's body ($m_2 = 0.92\ G$). In order to create the *VGRF* curve, the sum of the cosine functions describing the forces created during the motion of the two parts of the runner's body was used. With properly selected parameters, the proposed model allows the *VGRF* curves generated during heel-strike and forefoot-strike running to be determined.

Most recreational runners, around 90–95%, are heel-strike runners [21–23]. In [24], it was reported that in a group of professional marathon runners, nearly 75% of runners, were also heel-strike runners. The heel-strike running style can be considered to be the most common running style. Despite this, as mentioned earlier, the existing models of the *VGRF* generated by running people are mainly related to forces generated by forefoot-strike runners without taking into account the differences in parameters between the *VGRFs* generated by heel-strike and forefoot-strike runners.

For a better understanding of loads generated during running, a series of laboratory tests of people running and measurements of vertical ground reaction forces (*VGRFs*) were performed. Acquired forces were analysed using fast Fourier transform (*FFT*) to illustrate the differences in the parameters of the *VGRFs* generated by forefoot-strike and heel-strike runners. In addition, the *VGRFs* were parametrised in order to find the relation between the frequency of running and the foot contact time with the ground as well as the relation between frequency of running and *VGRF* amplitude for different running technique. The paper also presents the author's proposal of the mathematical model for the *VGRF* generated by heel-strike runners.

The research results presented in the paper enable a more accurate simulation of vertical forces induced by runners and can increase the accuracy of estimation of the dynamic response of civil engineering structures.

2. Materials and Methods

The *VGRFs* generated during running were measured during laboratory tests of a group of 13 healthy volunteers with full mobility and with no injuries and disabilities (5 males and 8 females, weight 51.6 ÷ 108.4 kg (mean ± SD: 70.2 ± 16.2 kg), height 158–187 cm (mean ± SD: 172.3 ± 9.8 m) age

22–45 years (mean ± SD: 25 ± 6.8 years)). Volunteers were chosen from the 22–45 age group using a convenience sampling method among students and employees of the University of Physical Education in Krakow and Cracow University of Technology.

All running tests were carried out in the laboratory of the Biomechanics Section of the University of Physical Education in Krakow. The force measurements were realized using two AMTI 6-degrees of freedom force plates (40×60 cm) located in line, one after the other, in the centre of a wooden walkway (Figure 2).
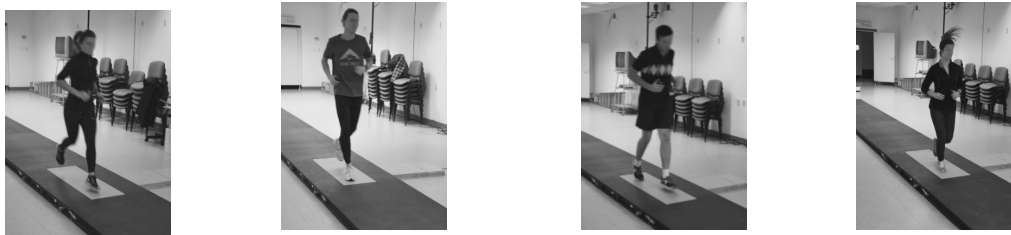

Figure 2. Running volunteers during the experiment (grey rectangle—the region of force measurement).

The data were collected at a sample rate of 1.0 kHz. A high sampling rate was necessary to accurately measure the impact peak of the *VGRF* generated by heel-strike runners.

During the tests, the volunteers ran in sports shoes. All test participants were asked to run at the pace indicated by the electronic metronome. The tests were performed in the frequency range 2.40–3.40 Hz to simulate slow, moderate and fast running pace. The running frequency increment was 0.2 Hz. The running frequencies were recalculated from [Hz] to [BPM] (beats per minute). The tested frequency range corresponds to the frequencies of the steps occurring during recreational and marathon running. Cases of very fast running or sprinting were not studied.

All volunteers were asked to land with their feet in the area of the force plates during the tests. Prior to conducting the force measurement, each volunteer practiced running with the frequency indicated by an electronic metronome to better match the running pace during the final measurement. All test participants performed two series of runs for each running frequency. The duration of each series was 60 s. After two series, the examined person rested during the series performed by other participants of the studies. The frequency was subsequently increased by 0.20 Hz, and the measurement was repeated for the new running frequency.

The recorded *VGRF* signals were filtered using a fourth-order low-pass Butterworth digital filter with a cut-off frequency of 60 Hz. The cut-off frequency of 60 Hz was established during signal processing tests as the frequency that allowed removal of unwanted noise and did not change the course of the *VGRF* waveform.

In analyses, the normalised (dimensionless) ground reaction forces F_{VGRF}, defined as $F_{VGRF} = VGRF/G$, were used (where: *VGRF*—recorded and filtered vertical component of the ground reaction force, *G*—weight of running person). To calculate the amplitudes of real *VGRF*, the amplitudes of normalised F_{VGRF} should be multiplied by the weight of running person *G*. The normalised F_{VGRF} forces were parameterised by the following indicators: the normalised amplitude of the impact peak (A_{ip}), the normalised amplitude of the propulsive peak ($A_{pp,h}$ or $A_{pp,f}$ for heel-strike and forefoot-strike runner respectively), the time of occurrence of A_{ip} (t_{ip}), the time of occurrence of $A_{pp,h}$ or $A_{pp,f}$ ($t_{pp,h}$ or $t_{pp,f}$) and the approximated contact time of the foot with the ground ($t_{ca,h}$ or $t_{ca,f}$ for heel-strike and forefoot-strike runner respectively, see Figure 1).

The times t_{ip}, $t_{pp,h}$ and $t_{pp,f}$ associated with the force curve peaks were extracted by finding the force curve peaks in the selected region of the curve along with the time values corresponding to identified peaks.

The approximated contact time of the foot with the ground, $t_{ca,h}$ or $t_{ca,f}$ (the time indicated by a dashed line in Figure 1), was obtained from the analysis of the collected data using the method

developed by the author. The approximated contact time was determined as the point of intersection of the time axis with a straight line passing through two points lying on the right half of the F_{VGRF} curve at the height corresponding to the value of the force amplitudes $F_{VGRF} = 1.0$ and $F_{VGRF} = 1.10$ (the origin of the coordinate system was taken at the beginning of the F_{VGRF} curve; $F_{VGRF} = 1.0$ corresponds to the body weight of the runner). This method allowed a straight line approximating the slope of the right half of the F_{VGRF} curve and the value of the approximated contact time of the foot with the ground to be determined. The approximated contact time was assumed as a curve indicator due to the method of force modelling (sinusoidal model), which precludes reconstruction of the actual curvature of the F_{VGRF} curve in its final part. The omitted low values of the F_{VGRF} were assumed negligible from the point of view of the dynamic analyses of building structures.

In order to determine the amplitude and phase spectra of the F_{VGRF} generated by heel-strike and forefoot-strike runners, the F_{VGRF} were decomposed using the fast Fourier transform (*FFT*). Each F_{VGRF} curve was analysed separately. Recorded steps were not organised into a set of successive steps. The duration of each of the analysed F_{VGRF} curves was assumed to be equal to the running period $T_r = 1/f_r$ (during the flight phase of running $F_{VGRF} = 0$ was assumed). The presented *FFT* results relate to the F_{VGRF} generated during running with a step frequency of $f_r = 2.80$ Hz, which can be assumed as the frequency of running at a normal pace [25–27].

Data recorded for heel-strike runners were used to develop the author's proposal of a load model describing the *VGRF* generated during heel-strike running. The function describing the impact peak occurring during heel-strike running was elaborated by analysing the variability of the parameter of the impact-peaks (amplitude and time of its occurrence). Due to a relatively large intra- and inter-subject variability of the analysed parameters, recommended values of the impact peak function parameters were presented in the form of ranges of values independent of the running frequency.

3. Results

In Tables 1–3 and in Figures 3 and 4, the results of the parameterisation of the F_{VGRF} generated by heel-strike and forefoot-strike runners are presented. In Figures 3 and 4, the regression lines and their equations are additionally presented (the bars in the charts represent the standard deviation).

Table 1. $A_{pp,h}$, $A_{pp,f}$, $t_{pp,h}$, $t_{pp,f}$ indicators of the F_{VGRF} curve (mean ± standard deviation).

Step Frequency [Hz]	Heel-Strike Runners		Forefoot-Strike Runners	
	$A_{pp,h} \pm SD$	$t_{pp,h} \pm SD$ [s]	$A_{pp,f} \pm SD$	$t_{pp,f} \pm SD$ [s]
2.4	2.047 ± 0.178	0.153 ± 0.012	2.300 ± 0.127	0.125 ± 0.013
2.6	2.155 ± 0.171	0.134 ± 0.011	2.385 ± 0.124	0.114 ± 0.011
2.8	2.203 ± 0.192	0.122 ± 0.014	2.488 ± 0.155	0.104 ± 0.012
3.0	2.180 ± 0.176	0.113 ± 0.013	2.453 ± 0.059	0.102 ± 0.010
3.2	2.098 ± 0.181	0.107 ± 0.009	2.450 ± 0.078	0.095 ± 0.011
3.4	2.085 ± 0.191	0.103 ± 0.012	2.428 ± 0.153	0.096 ± 0.011

Table 2. $t_{ca,h}$, $t_{ca,f}$ indicators of the F_{VGRF} curve (mean ± standard deviation).

Step Frequency [Hz]	Heel-Strike Runners	Forefoot-Strike Runners
	$t_{ca,h} \pm SD$ [s]	$t_{ca,f} \pm SD$ [s]
2.4	0.320 ± 0.019	0.283 ± 0.009
2.6	0.281 ± 0.015	0.253 ± 0.006
2.8	0.254 ± 0.017	0.226 ± 0.005
3.0	0.240 ± 0.017	0.213 ± 0.006
3.2	0.235 ± 0.008	0.200 ± 0.005
3.4	0.222 ± 0.015	0.190 ± 0.006

Table 3. A_{ip}, t_{ip} indicators of the F_{VGRF} curve (mean ± standard deviation).

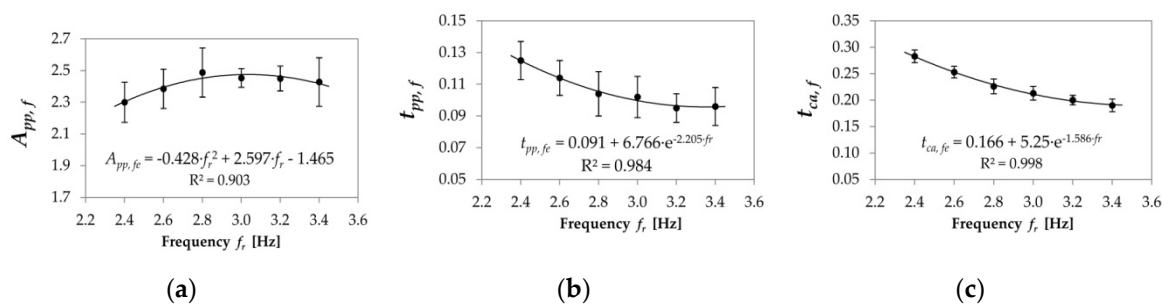| Step Frequency [Hz]	Heel-Strike Runners	
	$A_{ip} \pm SD$	$t_{ip} \pm SD$ [s]
2.4	1.245 ± 0.130	0.048 ± 0.008
2.6	1.311 ± 0.225	0.044 ± 0.008
2.8	1.280 ± 0.215	0.041 ± 0.006
3.0	1.255 ± 0.212	0.041 ± 0.008
3.2	1.345 ± 0.210	0.038 ± 0.007
3.4	1.346 ± 0.147	0.038 ± 0.005
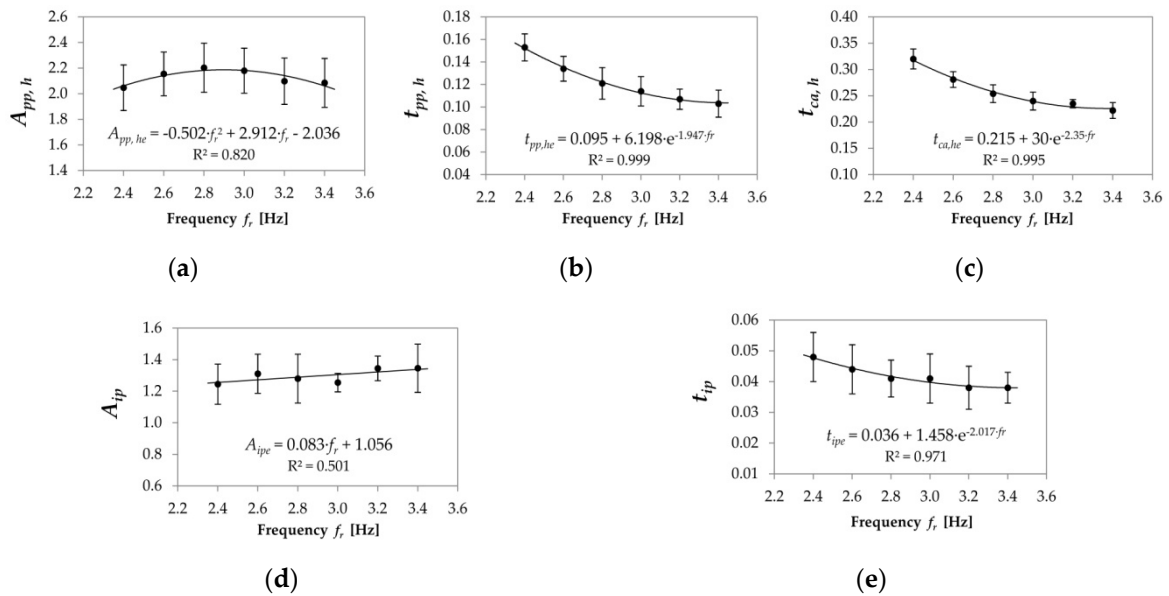
Figure 3. The F_{VGRF} curve indicators for heel-strike running style:(**a**) indicator $A_{pp,h}$, (**b**) indicator $t_{pp,h}$, (**c**) indicator $t_{ca,h}$, (**d**) indicator A_{ip}, (**e**) indicator t_{ip}.

Figure 4. The F_{VGRF} curve indicators for forefoot-strike running style: (**a**) indicator $A_{pp,f}$, (**b**) indicator $t_{pp,f}$, (**c**) indicator $t_{ca,f}$.

In Figures 5 and 6 the sample charts of the F_{VGRF} curves generated by heel-strike and forefoot-strike runners, respectively, along with the corresponding amplitudes and phase angles of fifteen harmonics are presented.
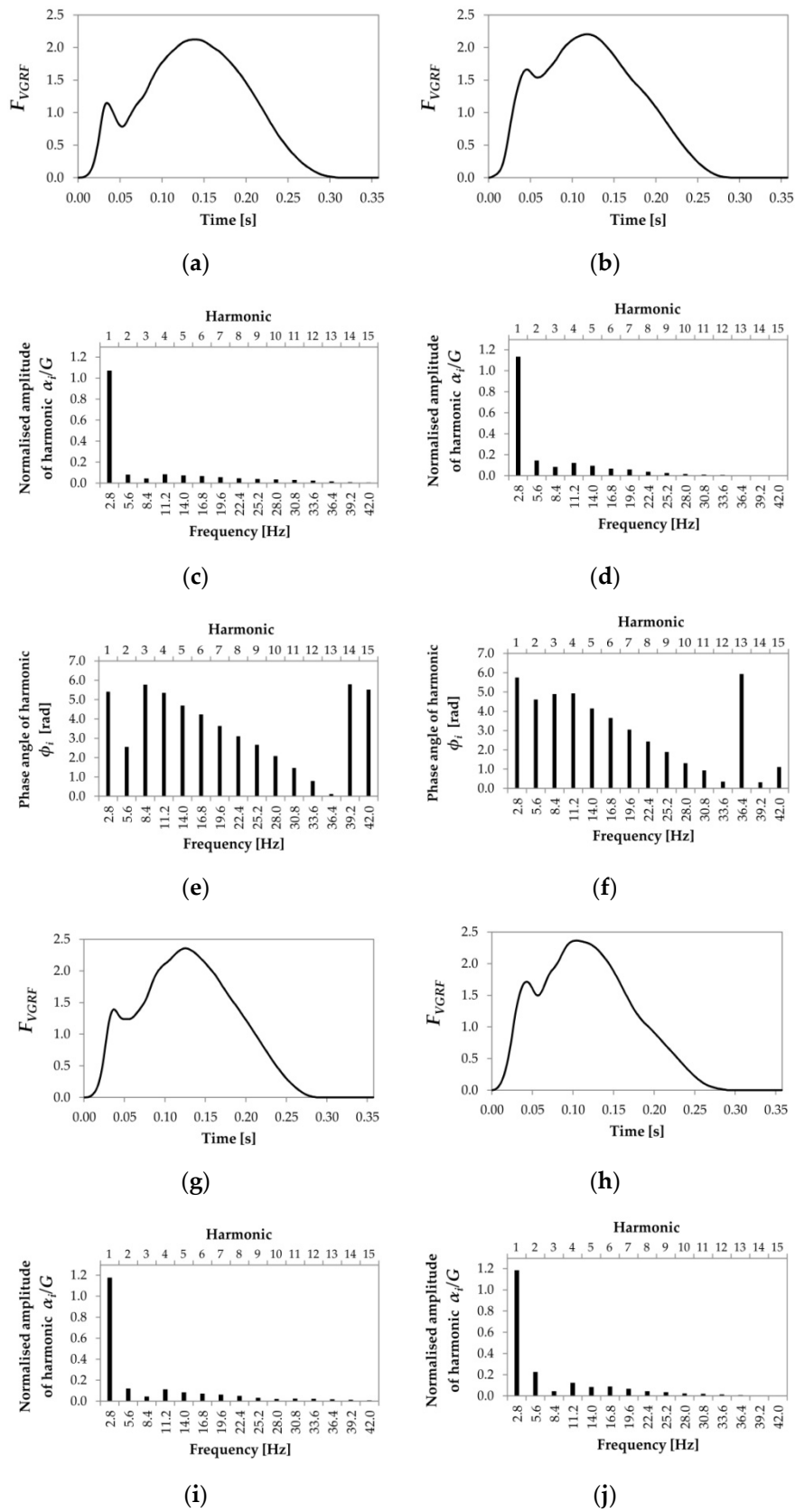
(**a**)

(**b**)

(**c**)

(**d**)

(**e**)

(**f**)

(**g**)

(**h**)

(**i**)

(**j**)

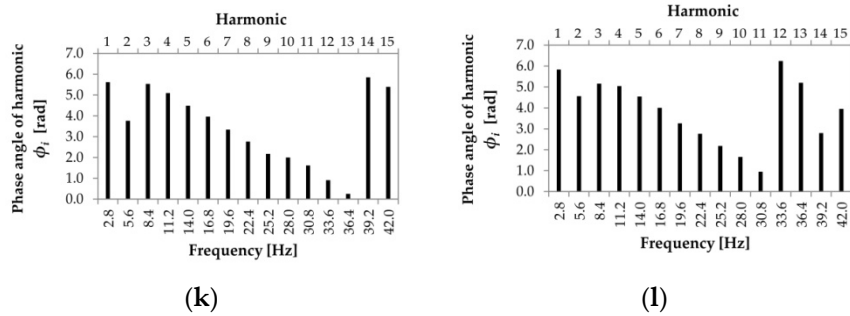**Figure 5.** *Cont.*

(**k**)

(**l**)

Figure 5. Sample charts of the F_{VGRF} curves generated by heel-strike runners ($f_r = 2.80$ Hz) and their corresponding amplitudes and phase angles for 15 harmonics: (**a,b,g,h**) examples of the F_{VGRF} curves; (**c,d,i,j**) normalised amplitudes of the F_{VGRF} harmonics; (**e,f,k,l**) phase angles of the F_{VGRF} harmonics (The data presented can be found in Supplementary Materials in the form of text files containing numerical data. See section Supplementary Materials).
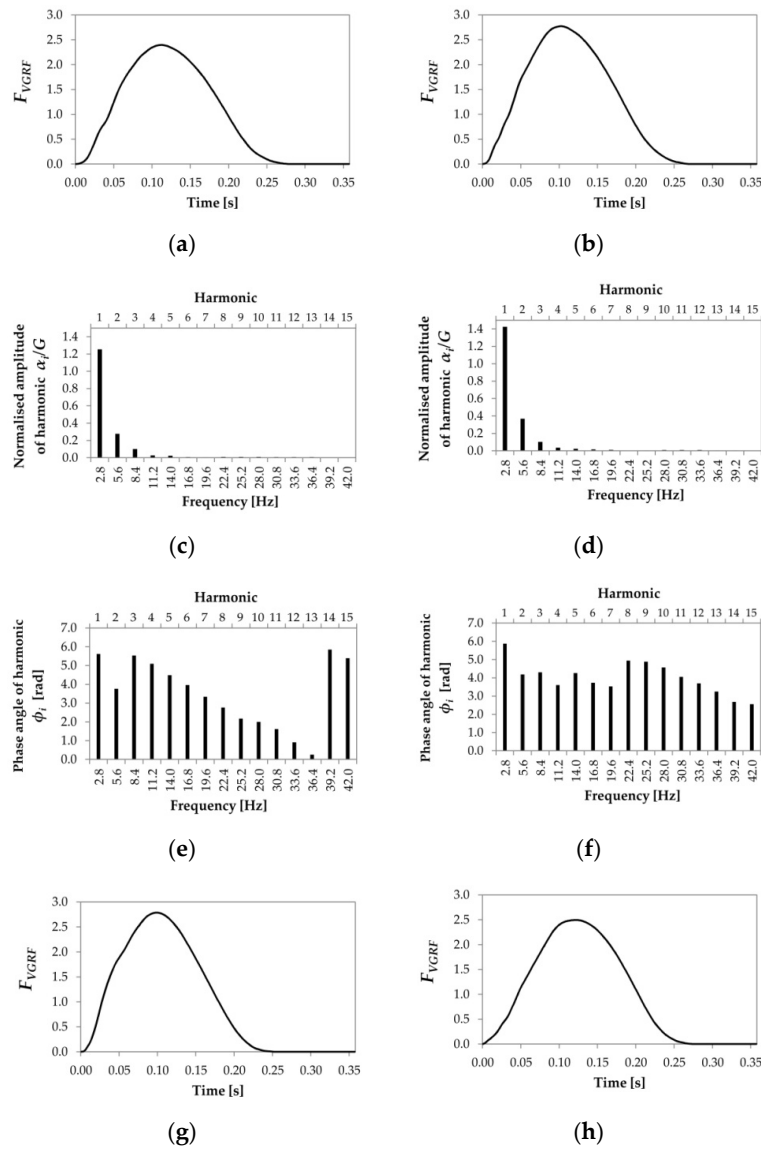

(**a**)

(**b**)

(**c**)

(**d**)

(**e**)

(**f**)

(**g**)

(**h**)

Figure 6. *Cont.*
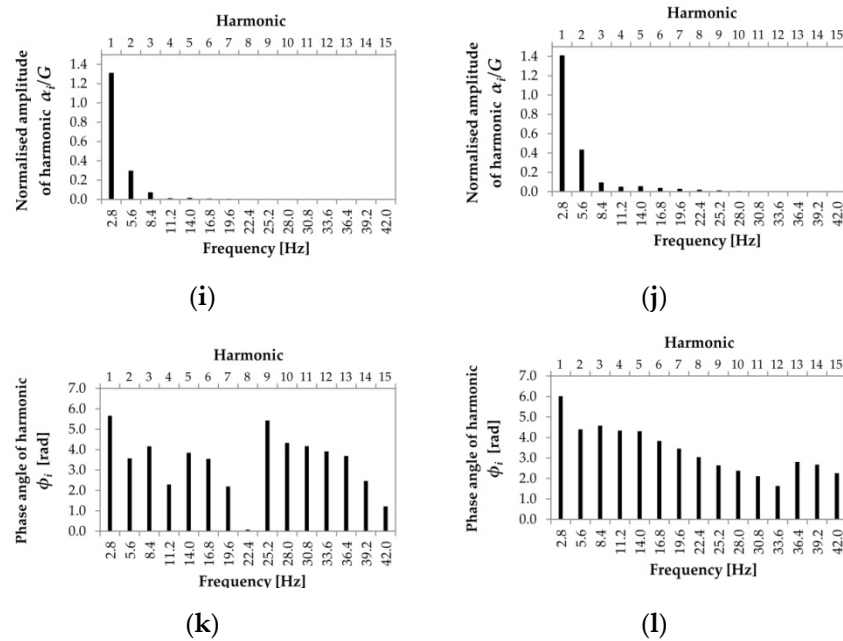
(i)

(j)

(k)

(l)

Figure 6. Sample charts of the F_{VGRF} curves generated by forefoot-strike runners (f_r = 2.80 Hz) and their corresponding amplitudes and phase angles for 15 harmonics: (**a**,**b**,**g**,**h**) examples of the F_{VGRF} curves; (**c**,**d**,**i**,**j**) normalised amplitudes of the F_{VGRF} harmonics; (**e**,**f**,**k**,**l**) phase angles of the F_{VGRF} harmonics (The data presented can be found in Supplementary Materials in the form of text files containing numerical data. See section Supplementary Materials).

Figures 7 and 8 present examples of normalised amplitudes and their corresponding phase angles of the fifteen F_{VGRF} harmonics determined for forty F_{VGRF} samples generated by four heel-strike and four forefoot-strike runners respectively. To improve the readability of the F_{VGRF} amplitudes of higher harmonics, the logarithmic scale of the F_{VGRF} amplitude charts is used (in Figures 5 and 6 the exemplary amplitudes of the F_{VGRF} curves in linear scale are presented).
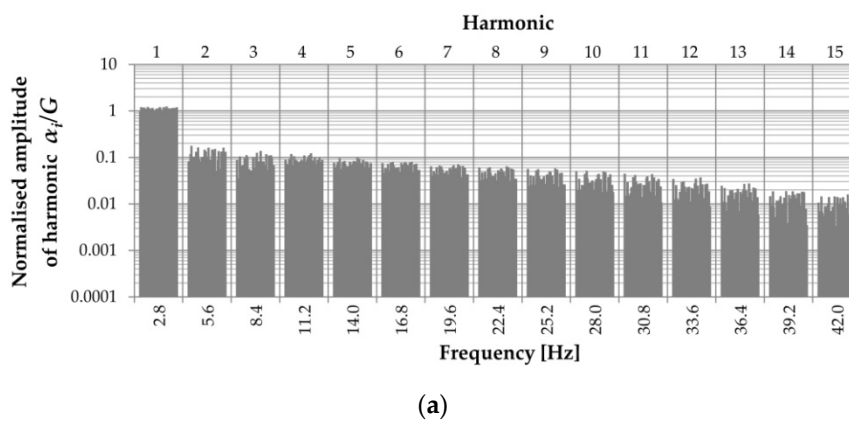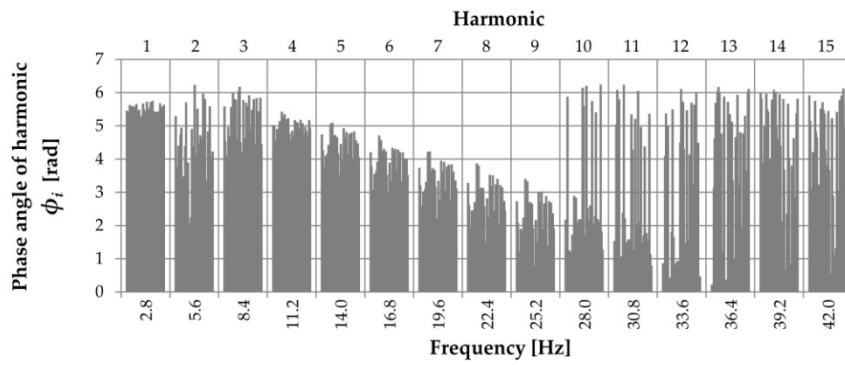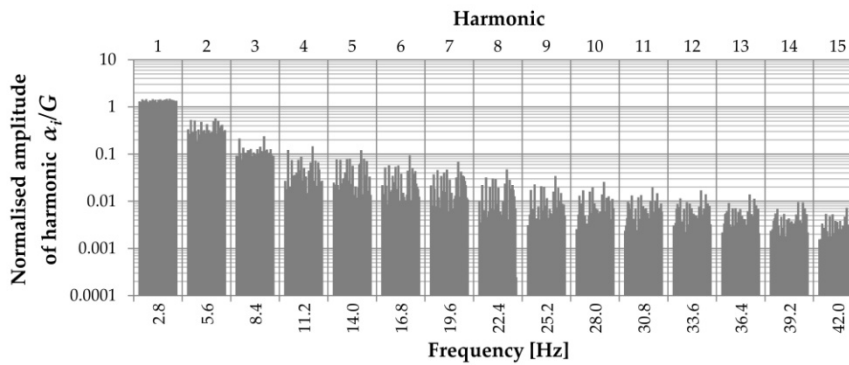

(a)

Figure 7. *Cont.*

Figure 7. The charts of (**a**) normalised amplitudes (log scale for the ϕ_i-axis) and (**b**) phase angles (linear scale for both axis) of the fifteen harmonics determined for forty F_{VGRF} samples generated by four heel-strike runners (f_r = 2.80 Hz) (The data presented can be found in Supplementary Materials in the form of text files containing numerical data. See section Supplementary Materials).
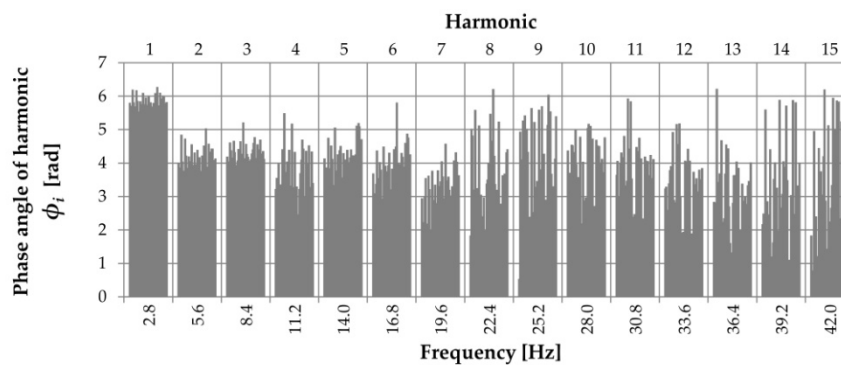

Figure 8. The charts of (**a**) normalised amplitudes (log scale for the ϕ_i-axis) and (**b**) phase angles (linear scale for both axis) of the fifteen harmonics determined for forty F_{VGRF} samples generated by four forefoot-strike runners (f_r = 2.80 Hz) (The data presented can be found in Supplementary Materials in the form of text files containing numerical data. See section Supplementary Materials).

4. Discussion

Section 3 presents the results of research on the vertical component of the ground reaction forces generated by running people (*VGRF*). The research took account of two different running styles: heel-strike running and forefoot-strike running. To the best of the author's knowledge, previous work

presenting the results of a similar study do not take into account the division of *VGRF* into different running styles. The presented analyses enabled the identification of the main features and differences between the *VGRF* generated as a result of two different running styles.

Comparing the amplitudes of the propulsive peaks $A_{pp,h}$ and $A_{pp,f}$ (Table 1, Figures 3a and 4a) and the values of the contact time of the foot with the ground $t_{ca,h}$, $t_{ca,f}$ (Table 2, Figures 3c and 4c), two main differences between heel-strike and forefoot-strike F_{VGRF} can be observed. Firstly, the mean F_{VGRF} amplitudes generated during forefoot-strike running ($A_{pp,f}$) reach values around 10–15% greater than the mean F_{VGRF} amplitudes generated during heel-strike running ($A_{pp,h}$). Secondly, the approximated contact time of the foot with the ground for forefoot-strike running ($t_{ca,f}$) is around 10–15% less than the approximated contact time for heel-strike running ($t_{ca,h}$). As confirmed by the results of analyses performed by the author, the use of accurate values of the contact time of the foot with the ground is crucial for proper modelling of the F_{VGRF} using the half-sine model presented in [7,13].

A similar relationship between the F_{VGRF} amplitudes generated during the normal pace of running (with a velocity of around 3.0 m/s) by forefoot-strike and heel-strike runners can be found in [28,29]. It was considered that results obtained by the author, which are consistent with the results presented in [28,29], indicate the relatively high importance of running technique for the F_{VGRF} amplitude. Further analyses of this topic are required.

The values of $t_{ca,h}$ and $t_{ca,f}$ can be estimated by empirical Formula (1) and (2):

$$t_{ca,he} = 0.215 + 30 \cdot e^{-2.35 \cdot f_r} \tag{1}$$

$$t_{ca,fe} = 0.166 + 5.25 \cdot e^{-1.586 \cdot f_r} \tag{2}$$

Equations (1) and (2) were determined by the author using an exponential regression line best fitted to the data set presented in Table 2 using the weighted nonlinear least-squares method. Fitted regression lines are shown in Figures 3c and 4c.

The use of Formula (1) and (2) allows the approximated contact times of the foot with the ground ($t_{ca,he}$, $t_{ca,fe}$) to be correctly estimated, and thus, the F_{VGRF} amplitudes for heel-strike and forefoot-strike running, respectively, can be correctly estimated. To compare the estimated F_{VGRF} amplitudes with the experimental values, in Table 4 the estimated values of amplitudes $A_{pp,he}$, $A_{pp,fe}$ determined for the estimated contact times $t_{ca,he}$, $t_{ca,fe}$ are presented. It can be seen that the estimated amplitudes are consistent with the experimental values of $A_{pp,h}$, $A_{pp,f}$ presented in Table 1. It is worth noting that the estimated amplitudes $A_{pp,he}$, $A_{pp,fe}$ are also consistent with the dynamic load factor k_p defined in [13]. However, it should be noted that according to the results obtained for the step frequency during running f_r in a range of 2.4–3.4 Hz, the mean value of the dynamic impact factor k_p defined in [13] as a function of t_c/T_r should be determined for the t_c/T_r ratio in a range of 0.63–0.77 (see the last two columns in Table 4, note: in the formula t_c/T_r use $t_{ca,he}$ or $t_{ca,fe}$ instead of t_c for heel-strike and forefoot-strike runners respectively). In addition, it is worth noting that the values of the contact duration of the foot with the ground presented in Table 2 are consistent with the recommendations presented in [13], after [30], only in the step frequency range f_r = 2.4–3.0 Hz. For $f_r > 3.0$ Hz, the values of the contact durations of the foot with the ground recommended in [13,28] are less than the experimental values presented in Table 2. Normalised force amplitudes determined for the shorter contact times of the foot with the ground, e.g., using the half-sine model, reach values of up to $F_{VGRF} \approx$ 3.0 that do not occur during the normal pace of the run (recreational running) [28,29]. These values can be considered the upper limit of the force amplitudes which can only occur during fast running at a speed of 5–6 m/s [28]. It is also worth noting that assuming the contact time $t_{ce} = 0.5\ T_r$, recommended in [7], leads to a constant and overestimated value of the F_{VGRF} amplitude for all step frequencies during running (see values of A_{ppe} in Table 4).

Table 4. Estimated parameters of the F_{VGRF} indicators.

Frequency f_r [Hz]	$t_{ca,he}$ [s] Equation (1)	$t_{ca,fe}$ [s] Equation (2)	$t_{ce} = 0.5$ T_r [s]	$A_{pp,he}$ (for $t_{ca,h}$)	$A_{pp,fe}$ (for $t_{ca,f}$)	A_{ppe} (for t_c)	$\frac{t_{ca,he}}{T_r}$	$\frac{t_{ca,fe}}{T_r}$
2.4	0.322	0.283	0.208	2.035	2.315	3.142	0.768	0.679
2.6	0.282	0.251	0.192	2.145	2.407	3.142	0.731	0.658
2.8	0.257	0.228	0.179	2.186	2.462	3.142	0.711	0.633
3.0	0.241	0.211	0.167	2.172	2.481	3.142	0.720	0.639
3.2	0.231	0.199	0.156	2.123	2.469	3.142	0.752	0.640
3.4	0.225	0.190	0.147	2.052	2.433	3.142	0.755	0.646

where: $T_r = 1/f_r$; $A_{pp,he}$, $A_{pp,fe}$, A_{ppe}—estimated amplitudes of normalised ground reaction forces F_{VGRF}: $A_{pp,he} = \pi/(2 \cdot t_{ca,he} \cdot f_r)$; $A_{pp,fe} = \pi/(2 \cdot t_{ca,fe} \cdot f_r)$; $A_{ppe} = \pi/(2 \cdot t_{ce} \cdot f_r)$ according to [7]. The amplitudes of the real *VGRFs* should be calculated as follows, e.g., $A_{pp,hR} = A_{pp,he} \cdot G$, $A_{pp,fR} = A_{pp,fe} \cdot G$, $A_{ppR} = A_{ppe} \cdot G$, where G—weight of running person.

Analysing the results presented in Tables 1 and 2 and in Figures 3 and 4, it can be observed that the F_{VGRF} amplitudes reach the highest values in the step frequency range of f_r = 2.70–3.10 Hz, which corresponds to a typical running pace.

Analysing the results presented in Figure 3d, the lack of an explicit trend of the impact peak indicator A_{ip} can be identified (large scatter of A_{ip} values). A linear regression was used to approximate the A_{ip} values. The mean value of the normalised amplitude of the impact peak is A_{ip} = 1.30. The impact peak A_{ip} occurs on average about 42.0 ms after the contact of the heel with the ground.

Analysing Figures 5–8, which show the normalised amplitudes of the F_{VGRF} harmonics (α_i/G, where: α_i—amplitude of the harmonic, G—weight of running person) generated during heel-strike and forefoot-strike running, it can be observed that the amplitude spectra for both running techniques are dominated by the amplitudes of the 1st harmonics with mean values and standard deviations of 1.08 ± 0.09 and 1.36 ± 0.07 for heel-strike and forefoot-strike running respectively. It can be also seen that the scatter of amplitudes of individual harmonics in the case of forefoot-strike running is greater than in the case of heel-strike running especially for higher harmonics (for $i \geq 4$, where: i—number of harmonic).

In the case of forefoot-strike running the 2nd harmonic reaches the mean value of around 24% of the amplitude of the 1st harmonic. The 3rd harmonic reaches a mean value of about 8% of the amplitude of the 1st harmonic. The mean amplitudes of the 4th and 5th harmonics reach around 2.5–2.7% of the amplitude of the 1st harmonic. The mean amplitudes of the 6th and 7th harmonics reach around 1.4–1.8% of the amplitude of the 1st harmonic. Higher harmonics (for $i \geq 8$) reach amplitudes of less than 1.0% of the amplitude of the 1st harmonic. A relatively fast decrease in the mean amplitude value of individual harmonics can be seen.

In the case of heel-strike running the distribution of normalised amplitudes of the analysed harmonics nos. 2–15 is more even than in the case of forefoot-strike running. A large number of harmonics reach amplitudes in the range of 4.0–9.0% of the amplitude of the 1st harmonic. The 2nd harmonic reaches a mean value of around 9% of the amplitude of the 1st harmonic. The 3rd harmonic reaches a mean value of around 7% of the amplitude of the 1st harmonic. The mean amplitudes of the 4th and 5th harmonics reach around 6.5–7.5% of the amplitude of the 1st harmonic. The mean amplitudes of the 6th and 7th harmonics reach about 4.6–5.6% of the amplitude of the 1st harmonic. The mean amplitudes of harmonics nos. 8–14 reach values in the range of 1.0–4.0% of the amplitude of the 1st harmonic.

Analysing the charts showing the phase angles of the F_{VGRF} harmonics (ϕ_i) presented in Figures 5–8, a relatively large scatter of the ϕ_i of individual harmonics can be noticed. This feature of the F_{VGRF} harmonics causes major problems in F_{VGRF} modelling using the Fourier series, especially in the case of the F_{VGRF} generated by heel-strike runners. The shape of the F_{VGRF} generated by forefoot-strike runners is dominated by the 1st harmonic and is slightly dependent on the values of the phase angles of the higher harmonics. Proper assumption of the phase angles for the first three harmonics is sufficient to correct modelling of the F_{VGRF} generated by forefoot-strike runners.

In the case of analysed running pace with a step frequency of f_r = 2.80 Hz the mean phase angles for the 1st harmonics of the F_{VGRF} are $\phi_{1,h}$ = 5.48 ± 0.13 rad (~1.75π) and $\phi_{1,f}$ = 5.83 ± 0.19 rad (~1.86π) for heel-strike and forefoot-strike running respectively. In the case of forefoot-strike running, the constant value of the phase angles $\phi_i \approx 4.0$ rad (~1.30π) for $i \geq 2$ can be assumed without significant loss of accuracy in determining the F_{VGRF} (compare Figure 8b).

In the case of the F_{VGRF} generated during heel-strike running, the characteristic is a large scatter of the phase angel values for the 2nd harmonic and almost linear decrease of the phase angles for harmonics 3–15 (Figure 7b). It should be noted that the reader should remember about the periodicity of the phase angles of ±2π (6.28 rad), which allows a large value of phase angles determined for higher harmonics (shown in Figure 7b for harmonics 10–15) to be converted to a small or negative value. The mean value and the standard deviation of the phase angle for the 2nd harmonic is ϕ_2 = 4.0 ± 1.15 rad. The value of the phase angle for the 3rd harmonic (ϕ_3) can be assumed to be in the range of 5.5–6.3 rad. The values of the phase angle for the higher harmonics (harmonics 4–15) should be linearly reduced every 0.5 rad (compare Figure 7c).

The constant term of the Fourier series (α_0) is another important parameter for modelling any curves by means of the Fourier series. This constant term α_0 represents the average value of the function over its domain. In the case of the F_{VGRF} generated by forefoot-strike runners the value of the normalised constant term can be assumed $\alpha_{0,f}$ = 1.0 ± 0.034. For the F_{VGRF} generated by heel-strike runners, the value of the normalised constant term is $\alpha_{0,h}$ = 0.978 ± 0.035.

Figure 9 presents the impact of the number of harmonics included in the F_{VGRF} modeling on the accuracy of the F_{VGRF} curve fitting. The residual plots, presented below the F_{VGRF} charts, show the accuracy of fitting of the F_{VGRF} to the example laboratory test result. To achieve high accuracy of the mapping of the F_{VGRF} curve generated by forefoot-strike runners, it is sufficient to use 3–5 harmonics (Figure 9e,f). In the case of the F_{VGRF} generated by heel-strike runners, sufficient accuracy can only be achieved if 10–15 harmonics are used (Figure 9c,d).
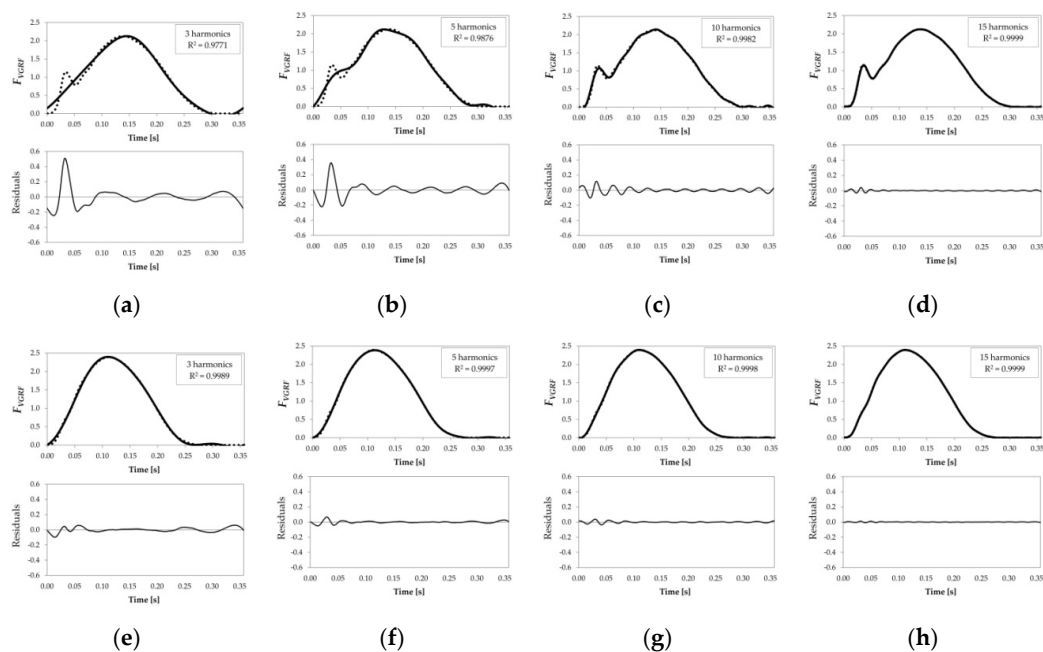

Figure 9. Impact of the number of harmonics on the accuracy of the F_{VGRF} curve modeling: (**a–d**) heel-strike running; (**e–h**) forefoot-strike running: (**a,e**) model containing 3 harmonics; (**b,f**) model containing 5 harmonics; (**c,g**) model containing 10 harmonics; (**d,h**) model containing 15 harmonics (upper chart—the F_{VGRF} curves, lower chart—residual plots; dot line—result of laboratory test, solid line—result of the F_{VGRF} fitting).

Due to the large variability of the Fourier series parameters, especially the phase angles values, modelling of the F_{VGRF} generated by heel-strike runners using the Fourier series can be burdensome and can lead to large inaccuracies. An alternative way of modelling of the F_{VGRF} generated by heel-strike runners should be proposed. This alternative method may be the method presented in [18–20]. This could also be the model proposed by the author and based on the half-sine model.

The F_{VGRF} generated by heel-strike runners can be simulated using the half-sine model (Equation (3) [7,13]) assuming the correct contact time value $t_{ca,he}$ according to Equation (2) and adding an impact peak function $\phi_{ip}(t)$ (Equation (6), author's proposal) responsible for producing the impact peak occurring in the F_{VGRF} generated by heel-strike runners.

$$F_{VGRF}(t) = \begin{cases} A_r \sin\left(\frac{\pi \cdot f_r}{k} \cdot t\right) & \text{for } i \cdot T_r < t \le (i+k) \cdot T_r \;\; i = 0, 1, 2 \ldots \\ 0 & \text{for } (i+k) \cdot T_r < t \le (i+1) \cdot T_r \end{cases} \tag{3}$$

$$k = \frac{t_{ca,he}}{T_r} \tag{4}$$

$$A_r = \frac{\pi}{2 \cdot k} \tag{5}$$

$$\frac{\phi_{ip}(t)}{G} = A_\phi \sin\left(\alpha_\phi \cdot \pi \cdot f_r \cdot t\right)^{\beta_\phi} \qquad \text{for} \quad 0 \le t \le \lambda \cdot T_r \tag{6}$$

where $F_{VGRF}(t)$—normalised vertical component of the ground reaction force $F_{VGRF}(t) = VGRF/G$, G—weight of running person (note: $VGRF(t) = F_{VGRF}(t) \cdot G$), A_r—the F_{VGRF} amplitude acc. to Equation (5), k—coefficient of contact time of the foot with the ground acc. to Equation (4), f_r—step frequency during running, T_r—step period during running $T_r = 1/f_r$, ϕ_{ip}—the impact peak function, A_ϕ—the impact peak amplitude, α_ϕ—coefficient of the impact peak location, β_ϕ—coefficient of the impact peak slenderness, λ—coefficient of the impact peak duration $\lambda \approx (0.17\text{–}0.20)T_r$ (only the first cycle of the impact peak function should be used).

During the analyses a large intra- and inter-subject variability of the impact peak parameters was observed, and for this reason, the recommended values of the impact peak parameters are presented in a form of ranges of values independent of the running frequency.

A typical A_ϕ value can be assumed to be in the range of 0.5–1.3. The value of the impact peak location coefficient α_ϕ can be assumed in the range $\alpha_\phi = 4$–8 (α_ϕ can be a decimal number). The coefficient α_ϕ should be adequately adjusted to the running frequency to achieve the location of the impact peak 30–45 ms after contact of the foot with the ground; $\alpha_\phi = 5$–8 or $\alpha_\phi = 4$–6 can be assumed for running frequency $f_r = 2.4$–2.8 Hz and $f_r = 2.8$–3.4 Hz respectively. $\beta_\phi = 2, 3, 4, 5,...$ can be assumed. The recommended value is $\beta_\phi = 4$ (β_ϕ can be a decimal number). For more information see [15].

In Figure 10 the F_{VGRF} generated using Equations (3)–(6) along with corresponding amplitude and phase angles spectra are presented.
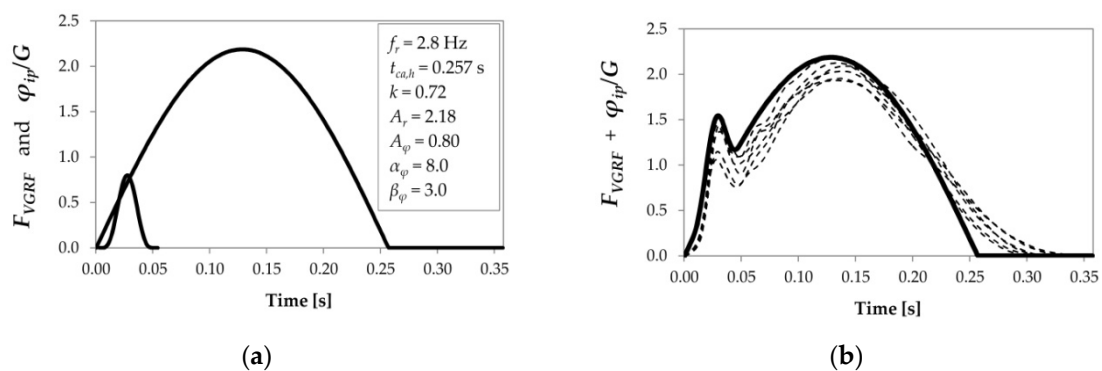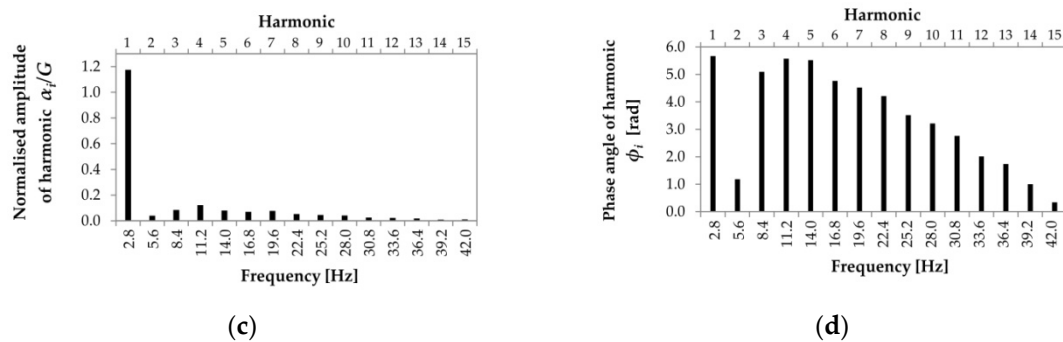

(a)

(b)

Figure 10. *Cont.*

(c) (d)

Figure 10. An example of an artificially generated vertical component of the ground reaction force for heel-strike running: (**a**) normalised ground reaction force F_{VGRF} generated using the half-sine model and normalised impact peak generated using the impact peak function, (**b**) the sum of normalised *VGRF* and normalised impact peak (solid bold line) in relation to the results of laboratory tests (thin dashed lines), (**c**) the amplitudes spectrum of the generated F_{VGRF}, (**d**) phase angles spectrum of the generated F_{VGRF}.

5. Summary

The paper presents the issue of the modelling of the vertical component of the ground reaction forces (*VGRF*) generated by running people. Two types of *VGRF* were analyzed related to two styles of running, i.e., heel-strike running and forefoot-strike running. This approach develops the current way of analysing the issue. The results of laboratory tests of runners allowed the formulation of new proposals for the description of the *VGRF* parameters. This helps to avoid overestimating the *VGRF* amplitude, increasing the accuracy of the *VGRF* determination and, as a consequence, increasing the accuracy of estimation of the dynamic response of the structure subjected to the dynamic action of runners. The presented results of analyses of two different types of forces generated during running can help engineers (structural designers) to better understand the principles and complexity of the *VGRF* modeling.

Supplementary Materials: Data presented in Figure 5a,b,g,h; Figure 6a,b,g,h; Figure 7a,b and Figure 8a,b are available online as supplementary material in a form of text files (.txt) at http://www.mdpi.com/2076-3417/10/5/1575/s1 (this web address must be edited).

Conflicts of Interest: The author declare no conflicts of interest.

References

1. Zäll, E.; Purroy, J.G.; Andersson, A.; Ülker-Kaustell, M. The effect of runners on footbridges—A case study. In *Proceedings of the 6th International Conference Footbridge 2017, Berlin, Germany, 6–9 September 2017*; Schlaich, M., Goldack, A., Eds.; Technische Universität Berlin: Berlin, Germany, 2017. [CrossRef]
2. Wang, C.; Shi, W. Optimal design and application of a multiple tuned mass damper system for an in-service footbridge. *Sustainability* **2019**, *1111*. [CrossRef]
3. Pańtak, M. Dynamic characteristics of medium span truss, cable-stayed and suspension steel footbridges under human-induced excitation. In *Proceedings of the 4th International Conference Footbridge 2011, Wrocław, Poland, 6–8 July 2011*; Biliszczuk, J., Bien, J., Hawryszkow, P., Kaminski, T., Eds.; Dolnośląskie Wydawnictwo Edukacyjne: Wroclaw, Poland, 2011.
4. Caetano, E.; Cunha, A.; Câncio Martins, L. Assessment of running pedestrian induced vibrations on a stress-ribbon footbridge. In *Proceedings of the 4th International Conference Footbridge 2011, Wrocław, Poland, 6–8 July 2011*; Biliszczuk, J., Bien, J., Hawryszkow, P., Kaminski, T., Eds.; Dolnośląskie Wydawnictwo Edukacyjne: Wroclaw, Poland, 2011.
5. Drygała, I.J.; Polak, M.A.; Dulińska, J.M. Vibration serviceability assessment of GFRP pedestrian bridges. *Eng. Struct.* **2019**, *184*, 176–185. [CrossRef]

6. Hawryszków, P. Dynamical investigation of a footbridge in Wronki near Poznań. In *Proceedings of the 8th International Conference on Arch Bridges ARCH 2016, Wrocław, Poland, 5–7 October 2016*; Biliszczuk, J., Bien, J., Hawryszkow, P., Kaminski, T., Eds.; Dolnośląskie Wydawnictwo Edukacyjne: Wroclaw, Poland, 2016; pp. 691–700.

7. Occhiuzzi, A.; Spizzuoco, M.; Ricciardelli, F. Loading models and response control of footbridges excited by running pedestrians. *Struct. Contr. Health Monit.* **2008**, *1515*, 349–368. [CrossRef]

8. Živanović, S. Vibration serviceability of a footbridge under vertical pedestrian load. In Proceedings of the 11th Symposium on Structural Dynamics and Vibration Measurement, Dubendorf, Switzerland, 30 May 2008.

9. Rainer, J.H.; Pernica, G. Vertical dynamic forces from footsteps. *Can. Acoust.* **1986**, *14*, 12–21.

10. Rainer, J.H.; Pernica, G.; Allen, D.E. Dynamic loading and response of footbridges. *Can. J. Civ. Eng.* **1988**, *1515*, 66–71. [CrossRef]

11. International Organization for Standardization. *Bases for Design of Structures—Serviceability of Buildings and Walkways Against Vibrations*; ISO 10137:2007; International Organization for Standardization: Geneva, Switzerland, 2007.

12. Bachmann, H.; Ammann, W.; Deischl, F.; Eisenmann, J.; Floegl, I.; Hirsch, G.H.; Klein, G.K.; Lande, G.J.; Mahrenholtz, O.; Natke, H.G.; et al. *Vibration Problems in Structures: Practical Guideline*; Birkhäuser Verlag: Basel, Switzerland, 1995.

13. Bachmann, H.; Ammann, W. *Vibrations in Structures Induced by Man and Machines*; IABSE: Zurich, Switzerland, 1987.

14. Feldmann, M.; Heinemeyer, C.; Lukić, M.; Caetano, E. *Human Induced Vibration of Steel Structure (HIVOSS): Background Document*; European Union: Luxembourg, 2008.

15. Pańtak, M. Runners on footbridges—A new *VGRF* model for heel strike running technique. *MATEC Web Conf.* **2019**, *262*, 64. [CrossRef]

16. Gruber, A.H.; Edwards, W.B.; Hamill, J.; Derrick, T.R.; Boyer, K.A. A comparison of the ground reaction force frequency content during rearfoot and non-rearfoot running patterns. *Gait Posture* **2017**, *56*, 54–59. [CrossRef] [PubMed]

17. Hamill, J.; Gruber, A.H. Is changing footstrike pattern beneficial to runners? *J. Sport Health Sci.* **2017**, *66*, 146–153. [CrossRef] [PubMed]

18. Racic, V.; Morin, J.B. Data-driven modelling of vertical dynamic excitation of bridges induced by people running. *Mech. Sys. Sig. Proc.* **2014**, *43*, 153–170. [CrossRef]

19. Clark, K.P.; Ryan, L.J.; Weyand, P.G. Foot speed, foot-strike and footwear: Linking gait mechanics and running ground reaction forces. *J. Exp. Biol.* **2014**, *217*, 2037–2040. [CrossRef] [PubMed]

20. Clark, K.P.; Ryan, L.J.; Weyand, P.G. A general relationship links gait mechanics and running ground reaction forces. *J. Exp. Biol.* **2017**, *220*, 247–258. [CrossRef] [PubMed]

21. Almeida, M.O.; Saragiotto, B.T.; Yamato, T.P.; Lopes, A.D. Is the rearfoot pattern the most frequently foot strike pattern among recreational shod distance runners? *Phys. Thera. Sport* **2015**, *16*, 29–33. [CrossRef] [PubMed]

22. Bakkie, D.; Mache, M.A.; Johnson, C.; Garcia-Krauss, P.; Kendall, K.; Hsieh, C. Foot strike pattern trends in sub-elite half marathon runners. In *Proceedings of the 31 International Conference on Biomechanics in Sports, Taipei, Taiwan, 07–11 July 2013*; University of Konstanz Open Journal Systems (OJS): Konstanz, Germany, 2013.

23. Larson, P.; Higgins, E.; Kaminski, J.; Decker, T.; Preble, J.; Lyons, D.; McIntyre, K.; Normile, A. Foot strike patterns of recreational and sub-elite runners in a long-distance road race. *J. Sports Sci.* **2011**, *2929*, 1665–1673. [CrossRef] [PubMed]

24. Hasegawa, H.; Yamauchi, T.; Kraemer, W.J. Foot strike patterns of runners at the 15-km point during an elite-level half marathon. *J. Str. Cond. Res.* **2007**, *2121*, 888–893. [CrossRef]

25. Hawryszków, P. Analysis of dynamical sensitivity and comfort of footbridges. In *Proceedings of the 4th International Conference Footbridge 2011, Wrocław, Poland, 6–8 July 2011*; Biliszczuk, J., Bien, J., Hawryszkow, P., Kaminski, T., Eds.; Dolnośląskie Wydawnictwo Edukacyjne: Wroclaw, Poland, 2011.

26. Hawryszków, P. Experimental vibration analysis of footbridges. In *Proceedings of the Conference EVACES 2013: Experimental Vibration Analysis for Civil Engineering Structures, 2013, Ouro Preto, Brazil, 28–30 October 2013*; Cury, A., Barbosa, F., Eds.; Even3: San Paulo, Brazil, 2017.

27. Živanović, S.; Pavic, A.; Reynolds, P. Vibration serviceability of footbridges under human-induced excitation: A literature review. *J. Sound. Vib.* **2005**, *279*, 1–74. [CrossRef]

28. Nilsson, J.; Thorstensson, A. Ground reaction forces at different speeds of human walking and running. *Acta Physiol. Scand.* **1989**, *136136*, 217–227. [CrossRef]

29. Keller, T.S.; Weisberger, A.M.; Ray, J.L.; Hasan, S.S.; Shiavi, R.G.; Spengler, D.M. Relationship between vertical ground reaction force and speed during walking, slow jogging, and running. *Clin. Biomech.* **1996**, *1111*, 253–259. [CrossRef]

30. Wheeler, J.E. Prediction and control of pedestrian-induced vibration in footbridges. *J. Str. Div.* **1982**, *108108*, 2045–2065.